Published in final edited form as:
Bone. 2011 October ; 49(4): 867–872. doi:10.1016/j.bone.2011.06.020.

Knee loading stimulates healing of mouse bone wounds in a femur neck

Ping Zhang[1,3] and **Hiroki Yokota**[2,3]

[1]Pediatrics, Indiana University School of Medicine, Indianapolis, IN 46202

[2]Biomedical Engineering, Indiana University Purdue University Indianapolis, IN 46202

[3]Anatomy and Cell Biology, Indiana University School of Medicine, Indianapolis, IN 46202

Abstract

Healing of bone wounds is sensitive to various environmental stimuli. Using knee loading, which has been shown to stimulate bone formation in mouse femora and tibiae, we addressed a question: Does knee loading accelerate a closure of open wounds in a femur neck? A surgical wound (0.5 mm in diameter) was generated at the femur neck in the left and right femora of C57/BL/6 female mice, and knee loading was applied to the left knee for 3 min/day for 3 consecutive days. Surgical holes at the femoral midshaft were used as control. Animals were sacrificed 1, 2, and 3 weeks after surgery for analyses with μCT and pQCT as well as mechanical testing. The results showed load-driven acceleration of the closure of surgical holes. Compared to a sham-loaded contralateral control, knee loading reduced the size of surgical wounds in the femoral midshaft by 14% ($p < 0.05$), 21% ($p < 0.01$), and 32% ($p < 0.001$) in 1, 2, and 3 weeks, respectively. It also decreased the wound size in the femur neck by 16% ($p < 0.001$; 1 week), 18% ($p < 0.001$; 2 weeks), and 21% ($p < 0.001$; 3 weeks). Images with pQCT revealed that bone mineral density (BMD) was increased from 571 ± 19 mg/cm^3 (control) to 686 ± 19 mg/cm^3 (loaded) ($p < 0.01$), and bone mineral content (BMC) from 3.05 ± 0.12 mg/mm (control) to 3.42 ± 0.11 mg/mm (loaded) ($p < 0.05$). Furthermore, mechanical testing showed that stiffness of the femur was increased by knee loading ($p < 0.05$). This study demonstrates that knee loading is capable of accelerating healing of surgical wounds throughout the femur including the femoral midshaft and neck.

Keywords

knee loading; wound healing; mouse; femur; femur neck

Introduction

Bone fracture occurs at multiple skeletal sites. Hip fractures are the third most frequent fractures next to vertebral and wrist fractures in the U.S., and the cost linked to hip fractures is the highest among all fracture types [1]. Although a total hip replacement is a well-

Corresponding Author: Hiroki Yokota, PhD, Department of Biomedical Engineering, Indiana University - Purdue University Indianapolis, SL220C, 723 West Michigan Street, Indianapolis, IN 46202, Phone: (317) 278-5177, Fax: (317) 278-2455, hyokota@iupui.edu.

The authors have no conflict of interest.

established surgical treatment, a non-invasive loading modality that could strengthen a femur and reduce a risk of hip fractures would be beneficial [2, 3]. In this study, we investigated potential effects of knee loading on strengthening the proximal femur and healing of bone wounds at the femur neck using a mouse model and examined a possibility of using knee loading for the prevention and supplementary treatment of hip fractures.

Knee loading is one form of joint loading modalities, in which lateral loads are applied to synovial joints such as the elbow [4], knee [5–7], and ankle [8]. Loads are compressive and typically sinusoidal, and are given for 3 to 5 min per day. In knee loading, lateral loads are given to the epiphyses of the femur and tibia in the mediolateral direction. In our previous studies we showed that the anabolic responses were detected both in the femur and tibia in 2 – 3 weeks after loading for 3 – 5 consecutive days [9, 10].

Induction of bone formation with knee loading is considered to be mediated by a cyclic change in intramedullary pressure in the femoral and tibial bone cavities. It is proposed that the load-driven pressure gradient generates fluid flow in a lacunocanalicular network in bone cortex and activates anabolic genes throughout the length of the femur and tibia [8, 11]. We have shown that knee loading stimulates bone formation by conducting bone histomorphometry using the cross-sections at 25% (distal femur), 50% (midshaft), and 75% (proximal femur) of the length of the femur, measured from the loading site at the knee [2, 3]. Our specific question herein was: Is knee loading able to induce bone formation and accelerate wound healing at the femur neck that is the remotest location from the loading site? Our hypothesis was that knee loading would enhance healing of surgical holes equally well both in the femoral midshaft and the femur neck.

To test the hypothesis, surgical holes were generated in the left and right femora either at the midshaft (50% site) or at the femur neck. The left femur received knee loading, while the right, contralateral femur was treated as a sham-loading control. We chose the surgical hole model, since it provided a reproducible experimental procedure with a well-defined quantitative measure through μCT imaging [12–14]. We also evaluated effects of knee loading on BMD and BMC using pQCT, and conducted mechanical testing for the estimation of overall stiffness of the femur.

Materials and methods

Animal preparation

Sixty-two C57BL/6 female mice (14 weeks of age) were obtained from Harlan Sprague-Dawley (Indianapolis, IN). Four to five mice were housed together in a cage, and mouse chow and water were given *ad libitum*. All procedures performed in this study were in accordance with the Indiana University Animal Care and Use Committee guidelines and were in compliance with the guiding principles in the care and use of animals endorsed by the American Physiological Society. Mice were allowed to acclimatize for 2 weeks before the experiment.

Surgical procedure

Animals received a surgical hole both in the left and right femora in the femoral diaphysis (midshaft; 25 mice) or the femur neck (37 mice). The animal was anesthetized with 2% isoflurane, and the hindlimb was shaved and sterilized with 10% providoneiodine solution. For the surgical wound in the femoral diaphysis, a 5-mm longitudinal skin incision was made over the anterior side of the hindlimb. A round surgical wound (0.5 mm in diameter), penetrating the anterior and posterior surfaces, was generated at a site ~ 7 mm proximal to the distal femoral end (50% along the length of the femur) (Fig. 1A & 1B) [14]. For the surgical wound in the femur neck, 5-mm longitudinal skin incision was made over the back

of the hindlimb (Fig. 1C). A hole of 0.5 mm in diameter was generated at the middle of the femur neck on the posterior cortex and the anterior cortex. A plunge router attachment was used to maintain stability and consistency of the operation. The muscles and skin were sutured and closed, and antibiotic prophylaxis (Enrofloxacin, 5 μg/g body mass) and analgesia (Morphine, 5 μg/g body mass) were administered for the first two postoperative days. Following the operation mice were allowed full unrestricted cage activity.

Mechanical loading

On days 4, 5 and 6 after surgery, knee loading was conducted to the left knee [2]. In brief, the mouse was anesthetized in an anesthetic induction chamber and then mask-anesthetized with 2% isoflurane. Using the custom-made piezoelectric loader, loads were applied in the lateral-medial direction for 3 minutes/day for 3 consecutive days at 15 Hz with a peak-to-peak force of 0.5 N (Fig. 1D). These loading conditions were chosen based on our previous mouse studies [2, 3]. The lateral and medial epicondyles of the femur together with the lateral and medial condyles of the tibia were in contact to the loader and the stator, respectively. The diameter of the loader and the stator was 5 mm, and they did not touch the surgical site. The right hindlimb was used as sham-loaded control, in which the right knee was placed under the loading rod in the same procedure without applying a voltage signal to the loader. Sham loading to the right limb was conducted immediately following the loading on the left limb.

Sample harvest

Animals were sacrificed for μCT and pQCT. The sample numbers were 10, 16, 17 and 19 in 0, 1, 2 and 3 weeks after surgery, respectively. Soft tissues were removed from the isolated femora, and the distal and proximal ends were cleaved to allow infiltration of the fixatives containing 10% neutral buffered formalin. After 48 h in the fixatives bones were transferred to 70% ethanol for storage.

Micro-computed tomography

Micro CT was performed using a desktop μCT-20 (Scanco Medical AG, Auenring, Switzerland). The harvested femur was placed in a plastic tube filled with 70% ethanol and centered in the gantry of the imaging device. A series of cross-sectional images were captured at 30-μm resolution using a medium resolution and bitmap images with 512 X 512 pixels were collected using 600 X-ray projections. The transverse and the axial sizes were estimated from 3D reconstructed images [14].

Peripheral quantitative computed tomography

The harvested femurs from seven mice (third postoperative weeks) were used for pQCT (XCT Research SA Plus, software 5.40; Norland-Stratec Medizintechnik GmbH, Birkenfel, Germany) [14]. The surgical wounds were scanned for five consecutive cross-sections with a sectional distance of 0.4 mm, where each section was 260 μm in thickness with a voxel size of 7 μm. For each slice, total volumetric bone mineral density ($vBMD_t$; mg/cm^3) and cortical bone mineral density ($vBMD_c$; mg/cm^3) were determined together with total bone area (A_t; mm^2) and cortical area (A_c; mm^2). From those data, total bone content ($vBMC_t = vBMD_t \times A_t$; mg/mm), and cortical bone content ($BMC_c = BMD_c \times A_c$; mg/mm) were derived. Prior to scanning soft tissues were removed and samples were scanned in air.

Mechanical testing

The harvested femurs from seven mice (third postoperative weeks) were used for mechanical testing. These were the same samples used for pQCT imaging. The bones were loaded to failure by four-point bending [15–19]. Prior to testing samples were rehydrated

overnight in 0.9% NaCl at room temperature. Testing was performed on a miniature materials testing machine (Vitrodyne V1000; Liveco, Inc., Burlington, VT, USA), which has a force resolution of 0.05 N. The crosshead speed during testing was 0.2 mm/s, and force-displacement data was collected every 0.01 s. From the data, a force-versus-displacement graph was generated and the ultimate force and displacement, stiffness, and energy to ultimate force were calculated.

Statistical analysis

The data were expressed as mean ± SEM. Statistical significance among groups was examined using one-way ANOVA. For pair-wise comparisons a post-hoc test was conducted using Fisher's protected least-significant-difference tests. A paired *t*-test was employed to evaluate statistical significance between the loaded samples and sham-loaded controls. All comparisons were two-tailed and statistical significance was assumed for $p < 0.05$. The single, double and triple asterisks in figures indicate $p < 0.05$, $p < 0.01$ and $p < 0.001$, respectively.

Results

No infections were detected at the surgical site during the 3-week course of experiments. We did not observe any abnormal behavior, weight loss, or diminished food intake.

Accelerated closure of surgical holes in the femoral diaphysis with knee loading

Micro CT images displayed an accelerated closure of the surgical hole in the femoral midshaft with knee loading (Fig. 2). We evaluated a wound closure by measuring the axial and lateral sizes of the anterior and posterior holes. During a 3-week period, the overall improvement of bone wound closure by knee loading was 14% (1 week, $p < 0.05$), 21% (2 weeks, $p < 0.01$), and 32% (3 weeks, $p < 0.001$), based on an average wound size of anterior and posterior holes.

The size of the wounds on the anterior cortex was decreased from 0.47 ± 0.01 mm (control) to 0.41 ± 0.01 mm (loaded; $p < 0.05$) in the first week, while the wounds on the posterior cortex were also reduced from 0.44 ± 0.02 mm (control) to 0.37 ± 0.01 mm (loaded; $p < 0.05$) (Fig. 3). In the second and third weeks, the wound size was further decreased and the decrease was statistically significant both on the anterior and posterior surfaces.

Interestingly, the wounds did not heal uniformly in the axial and transverse directions (Fig. 4). Three weeks after surgery, for instance, the wound size was 0.41 ± 0.01 mm (control) and 0.28 ± 0.01 mm (loaded, $p < 0.001$) in the axial direction, while 0.18 ± 0.01 mm (control) and 0.12 ± 0.01 mm (loaded, $p < 0.001$) in the transverse direction. Note that the wound size was defined as the mean values independently measured along the axial and transverse directions.

Accelerated closure of surgical holes in the femur neck with knee loading

Micro CT images also displayed an accelerated closure of the surgical hole in the femur neck by knee loading (Fig. 5). Knee loading reduced the size of surgical wounds by 16% from 0.41 ± 0.01 mm (control) to 0.34 ± 0.01 mm (loaded, $p < 0.001$) in the first postoperative week. The wound size was decreased by 18% in the second week from 0.39 ± 0.01 mm (control) to 0.32 ± 0.01 mm (loaded, $p < 0.001$), and by 21% in the third week from 0.37 ± 0.01 mm (control) to 0.29 ± 0.01 mm (loaded, $p < 0.001$).

Elevated BMD and BMC in the femoral midshaft with knee loading

Evaluation of bone quality with pQCT revealed that knee loading increased BMD and BMC at the wound site (Fig. 6). Total BMD was elevated by 20% from 571 ± 19 mg/cm^3 (control) to 686 ± 19 mg/cm^3 (loaded, $p < 0.01$), while cortical BMD was elevated by 6% form 1057 ± 19 mg/cm^3 (control) to 1136 ± 10 mg/cm^3 (loaded, $p < 0.01$). Furthermore, total BMC was 12% higher (3.05 ± 0.12 mg/mm in control samples and 3.42 ± 0.11 mg/mm in loaded samples; $p < 0.05$). An increase of 21% in cortical BMC was detected from 2.25 ± 0.11 mg/mm (control) to 2.73 ± 0.11 mg/mm (loaded, $p < 0.01$).

Increased stiffness with knee loading

Mechanical test showed that knee loading increased stiffness of the femur from 27.8 ± 1.9 N/mm (control) to 38.6 ± 4.4 N/mm (loaded) ($p < 0.05$) (Table 1). In concert with an increase in stiffness, ultimate force was higher and displacement at ultimate force was lower in the loaded femora than control samples although no statistical significance was obtained ($p = 0.23 – 0.30$).

Discussion

We demonstrate that laterally applied mechanical loads at the distal end of the femur are able to enhance bone formation and wound healing not only in the femoral midshaft but also at the femur neck. Micro CT images clearly reveal that knee loading accelerates a closure of the surgical hole in the femoral midshaft and neck. The knee-loaded holes in the femur neck were smaller than the contralateral holes by 16%, 18%, and 21% in the first, second, and third postoperative weeks, respectively. The results with pQCT and mechanical test show that knee loading increases BMD and BMC at the wound site and elevates overall stiffness of the femur. Thus, knee loading is apparently capable of activating anabolic responses throughout the femur.

For the surgical holes in the femoral midshaft and neck, knee loading is equally effective. Compared to the contralateral control, the reduction in the wound size by knee loading in the first operative week is 14% in the midshaft and 16% in the femur neck. Interestingly, loading effects are more predominant in the later operative weeks and this trend is observed both in the femoral midshaft and neck. For instance, the surgical holes in the femoral midshaft were smaller in the knee-loaded limb than the contralateral limb by 14%, 21%, and 32% in the first, second, and third operative weeks, respectively. The accelerated closure is detected in the anterior and posterior wounds, but the closure is quicker in the transverse direction than the axial direction. Knee loading also increases an overall stiffness of the femur in the third operative week, in good agreement with the elevation in BMD and BMC.

Knee loading is shown to be effective in inducing bone formation throughout the femur and tibia regardless of distance from the loading site in the knee. Loads of 0.5 N to the mouse knee, employed in this study, generates dynamic strain of 10 – 20 μstrain in the midshaft of the femur, and strain in the femur neck is expected to be at the same level [2]. To induce bone formation in the mouse tibia, a tibia axial (bending) modality typically requires ~ 12 N or more, while knee loading needs 0.5 N or less [20–22]. The measurements with a FRAP (fluorescence recovery after photo bleaching) technique indicate that knee loading stimulates molecular transport in the diaphyseal cortical bone of the mouse femur. Further, load-driven alteration of intramedullary pressure in the absence of surgical holes was detected using a fiber optic pressure sensor [23]. The observed pressure amplitude (half of peak-to-peak) in the femoral bone cavity ranged from 3 to 130 Pa depending on the loading conditions (0.5 to 4 N at 0.5 to 50 Hz), and the alteration was synchronous to loads applied with knee loading [11].

Although the current study is consistent with anabolic responses mediated by knee loading [2, 3], the presence of surgical holes herein presents a unique biophysical environment. We reported previously using an *ex vivo* mouse femur model that knee loading stimulated oscillatory movements of microparticles in a glass tube connected to a surgical hole [11]. Further, we showed that in response to knee loading a surgical hole in the tibia reduced load-driven bone formation in the tibia [6]. Taken together, the hole would act as a pressure sink and our working hypothesis is that load-driven intramedullary flow would stimulate transport of fluid in a bone cavity consisting of bone-marrow derived stem cells at the injury site. To evaluate this potential mechanism, it is necessary to determine a pattern of cell migration and characterize the type of tissues formed during the healing process at the injury site.

To examine efficacy of knee loading at the femur neck, we employed a surgical wound model. No single small animal model is adequate to fully evaluate efficacy and safety of knee loading and the current study is the first step to develop a clinically relevant strategy. Although this model did not represent a clinically relevant bone fracture, it provided a reproducible assay system to evaluate a proof of concept of the application of knee loading [14]. The model is well-established for studies on bone defect repair in normal and transgenic animals [12, 13, 24, 25]. The surgical wounds can be generated bilaterally (two wounds in a single femur) and allow us the comparison of a healing process in two femoral surfaces.

There are other forms of mechanical loading such as joint rotation [26, 27], and whole-body and local vibrations [28, 29]. To our knowledge, however, no loading modality has been clinically applied for treatment of a femur neck or head. By developing a loading device for human use, knee loading might potentially be used as a preventive procedure to reduce a risk of hip fracture and a supplementary treatment to enhance fracture healing. It is important to evaluate proper loading conditions for human use, and these conditions may depend on types of fractures such as closed and non-union fractures. In summary, knee loading is capable of inducing bone formation and accelerating wound healing throughout the femur including surgical holes in the femur neck.

Highlights

- Knee loading is reported to stimulate bone formation in the femur and tibia.
- Here, knee loading is shown to accelerate a closure of open wounds in a femoral midshaft and neck.
- Images with pQCT reveal that bone mineral density is elevated.
- Mechanical testing shows that stiffness of the femur is increased.

Acknowledgments

This study was supported by grants from the National Institute of Arthritis and Musculoskeletal and Skin Diseases Grant R03AR55322 (to P. Zhang) and R01AR52144 (to H. Yokota).

REFERENCES

1. Burge R, Dawson-Hughes B, Solomon DH, Wong JB, King A, Tosteson A. Incidence and economic burden of osteoporosis-related fractures in the United States, 2005–2025. J Bone Miner Res. 2007; 22:465–475. [PubMed: 17144789]
2. Zhang P, Su M, Tanaka S, Yokota H. Knee loading causes diaphyseal cortical bone formation in murine femurs. BMC Musculoskel Dis. 2006; 73:1–12.

3. Zhang P, Tanaka S, Sun Q, Turner CH, Yokota H. Frequency-dependent enhancement of bone formation in murine tibiae and femora with knee loading. J Bone Miner Metab. 2007; 25:383–391. [PubMed: 17968490]
4. Yokota H, Tanaka SM. Osteogenic potentials with joint loading modality. J Bone Miner Metab. 2005; 23:302–308. [PubMed: 15981026]
5. Zhang P, Tanaka SM, Jiang H, Su M, Yokota H. Diaphyseal bone formation in murine tibiae in response to knee loading. J Appl Physiol. 2006; 100:1452–1459. [PubMed: 16410382]
6. Zhang P, Yokota H. Effects of surgical holes in mouse tibiae on bone formation induced by knee loading. Bone. 2007; 40:1320–1328. [PubMed: 17344109]
7. Zhang P, Hamamura K, Turner CH, Yokota H. Lengthening of mouse hindlimbs with joint loading. J Bone Miner Metab. 2010; 28:268–275. [PubMed: 19890688]
8. Zhang P, Turner CH, Yokota H. Joint loading-driven bone formation and signaling pathways predicted from genome-wide expression profiles. Bone. 2009; 44:989–998. [PubMed: 19442616]
9. Zhang P, Malacinski GM, Yokota. Joint Loading Modality: Its Application to Bone Formation and Fracture Healing. Br J Sport Med. 2008; 42:556–560.
10. Zhang P, Hamamura K, Yokota H, Malacinski GM. Potential applications of pulsating joint loading in sports medicine. Exerc Sport Sci Rev. 2009; 37:52–56. [PubMed: 19098525]
11. Zhang P, Su M, Liu Y, Hus A, Yokota H. Knee loading dynamically alters intramedullary pressure in mouse femora. Bone. 2007; 40:538–543. [PubMed: 17070127]
12. He YX, Zhang G, Pan XH, Liu Z, Zheng LZ, Chan CW, et al. Impaired bone healing pattern in mice with ovariectomy-induced osteoporosis: A drill-hole defect model. Bone. 2011 [Epub ahead of print].
13. Monfoulet L, Malaval L, Aubin JE, Rittling SR, Gadeau AP, Fricain JC, et al. Bone sialoprotein, but not osteopontin, deficiency impairs the mineralization of regenerating bone during cortical defect healing. Bone. 2010; 46:447–452. [PubMed: 19761880]
14. Zhang P, Sun Q, Turner CH, Yokota H. Knee loading accelerates bone healing in mice. J Bone Miner Res. 2007; 22:1979–1987. [PubMed: 17696761]
15. Sun Q, Alam I, Liu L, Koller DL, Carr LG, Econs MJ, et al. Genetic loci affecting bone structure and strength in inbred COP and DA rats. Bone. 2008; 42:547–553. [PubMed: 18158281]
16. Schriefer JL, Robling AG, Wanden SJ, Fournier AJ, Mason JJ, Turner CH. A comparison of mechanical properties derived from multiple skeletal sites in mice. J Biomech. 2005; 38:467–475. [PubMed: 15652544]
17. Wallace JM, Rajachar RM, Allen MR, Bloomfield SA, Robey PG, Young MF, et al. Exercise-induced changes in the cortical bone of growing mice are bone- and gender-specific. Bone. 2007; 40:1120–1127. [PubMed: 17240210]
18. Volkman SK, Galecki AT, Burke DT, Miller RA, Goldstein SA. Quantitative trait loci that modulate femoral mechanical properties in a genetically heterogeneous mouse population. J Bone Miner Res. 2004; 19:1497–1505. [PubMed: 15312250]
19. Balooch G, Balooch M, Nalla RK, Schilling S, Filvaroff EH, Marshall GW, et al. TGF-beta regulates the mechanical properties and composition of bone matrix. Proc Natl Acad Sci USA. 2005; 102:18813–18818. [PubMed: 16354837]
20. LaMothe JM, Hamilton NH, Zernicke RF. Strain rate influences periosteal adaptation in mature bone. Med Eng Phys. 2005; 27:277–284. [PubMed: 15823468]
21. Kesavan C, Mohan S, Srivastava AK, Kapoor S, Wergedal JE, Yu H, et al. Identification of genetic loci that regulate bone adaptive response to mechanical loading in C57BL/6J and C3H/HeJ mice intercross. Bone. 2006; 39:634–643. [PubMed: 16713414]
22. De Souza RL, Matsuura M, Eckstein F, Rawlinson SC, Lanyon LE, Pitsillides AA. Non-invasive axial loading of mouse tibiae increases cortical bone formation and modifies trabecular organization: a new model to study cortical and cancellous compartments in a single loaded element. Bone. 2005; 37:810–818. [PubMed: 16198164]
23. Su M, Jiang H, Zhang P, Liu Y, Wang E, Hsu A, et al. Load-driven molecular transport in mouse femur with knee-loading modality. Annals Biomed Eng. 2006; 34:1600–1606.

24. Usitalo H, Rantakokko J, Ahonen M, Jämsä T, Tuukkanen J, Kähäri VM, et al. A metaphyseal defect model of the femur for studies of murine bone healing. Bone. 2001; 28:423–429. [PubMed: 11336924]

25. Campbell TM, Wong WT, Mackie EJ. Establishment of a model of cortical bone repair in mice. Calcif Tissue Int. 2003; 73:49–55. [PubMed: 14506954]

26. Gu XI, Leong DJ, Guzman F, Mahamud R, Li YH, Majeska RJ, Schaffler MB, Sun HB, Cardoso L. Development and validation of a motion and loading system for a rat knee joint *in vivo*. Annals Biomed Eng. 2010; 38:621–631.

27. Leong DJ, Gu XI, Li Y, Lee JY, Laudier DM, Majeska RJ, Schaffler MB, Cardoso L, Sun HB. Matrix metalloproteinase-3 in articular cartilage is upregulated by joint immobilization and suppressed by passive joint motion. Matrix Biol. 2010; 29:420–426. [PubMed: 20153826]

28. Rubin C, Recker R, Cullen D, Ryaby J, McCabe J, McLeod K. Prevention of postmenopausal bone loss by a low-magnitude, high-frequency mechanical stimuli: a clinical trial assessing compliance, efficacy, and safety. J Bone Miner Res. 2004; 19:343–351. [PubMed: 15040821]

29. Leung KS, Shi HF, Cheung WH, Qin L, Ng WK, Tam KF, Tang N. Low-magnitude high-frequency vibration accelerates callus formation, mineralization, and fracture healing in rats. J Orthop Res. 2009; 27:458–465. [PubMed: 18924140]

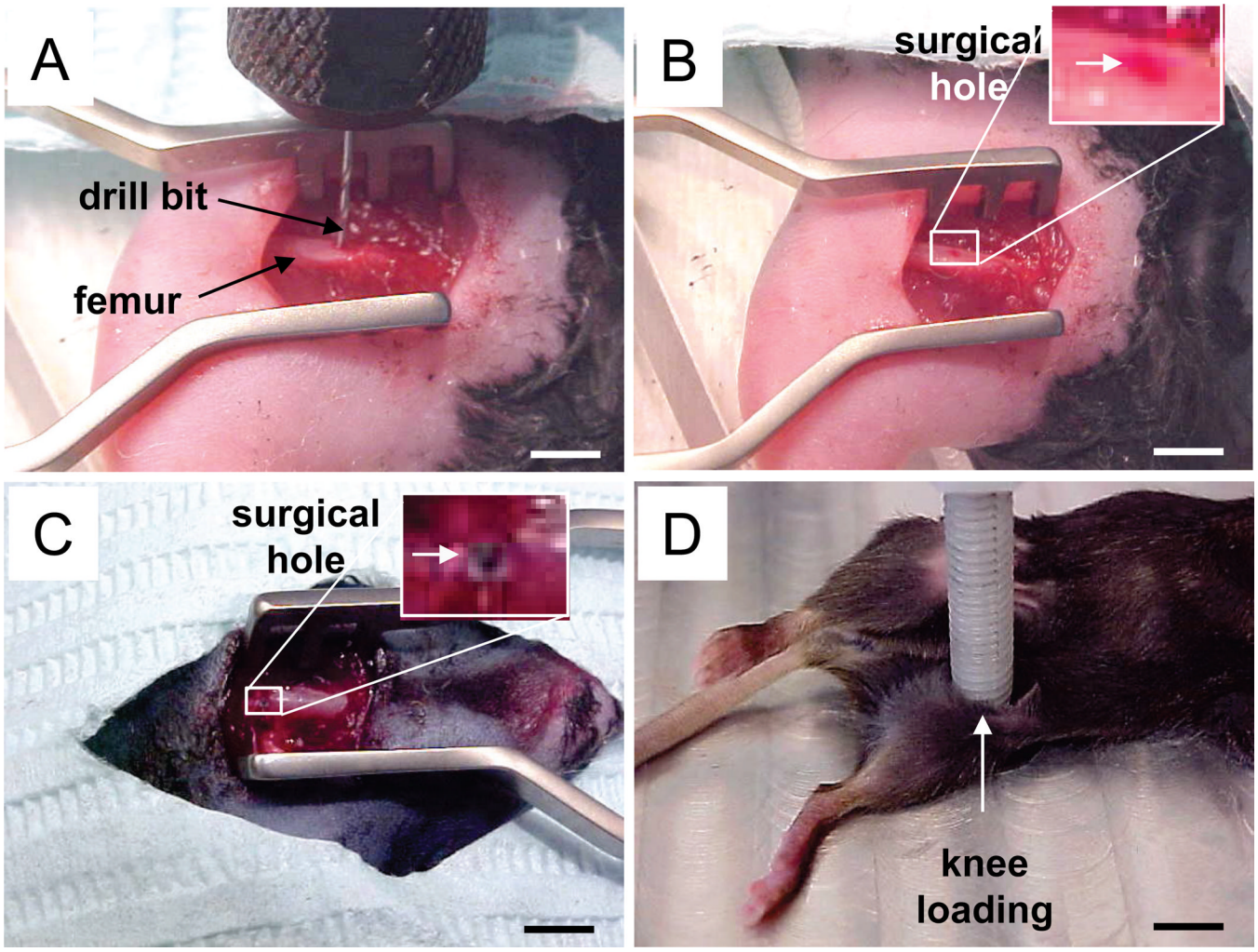

Figure 1.
The surgical and loading procedure. (A) A drill bit on the middle of femur. Bar = 2 mm. (B) Femoral diaphysis with a surgical hole. Bar = 2 mm. (C) Left femur neck with a surgical hole. Bar = 2 mm. (D) Left knee on a loading table for knee loading on the fourth postoperative day. Bar = 4 mm.

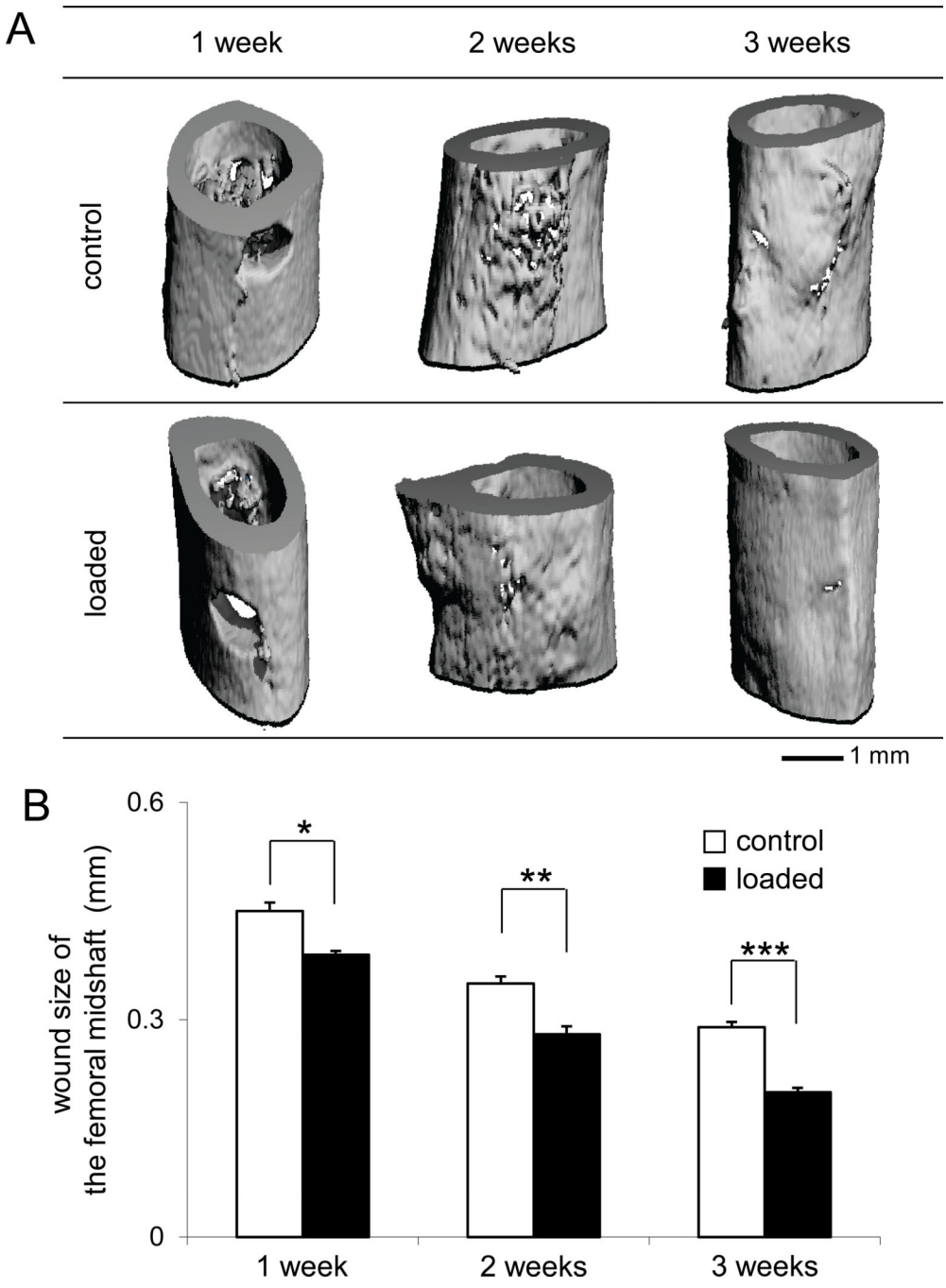

Figure 2.

Surgical wounds in the femoral midshaft. (A) Micro CT images of the surgical holes in the control and loaded femora in 1, 2, and 3 weeks after surgery. (B) Changes in wound size in the femoral midshaft (mm).

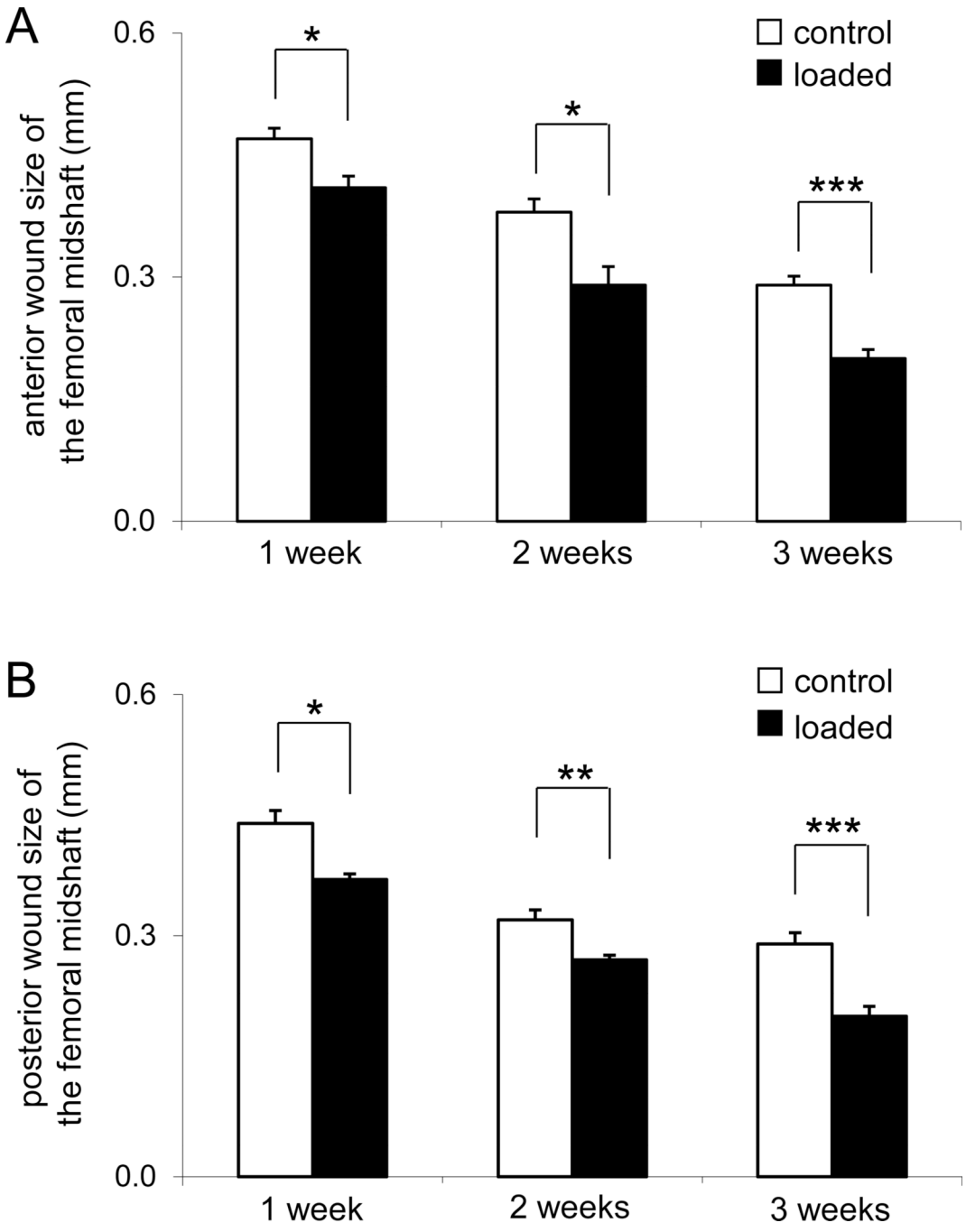

Figure 3.
Alterations in anterior and posterior wound size in the femoral midshaft. (A) Wound size on the anterior surface (mm). (B) Wound size on the posterior surface (mm).

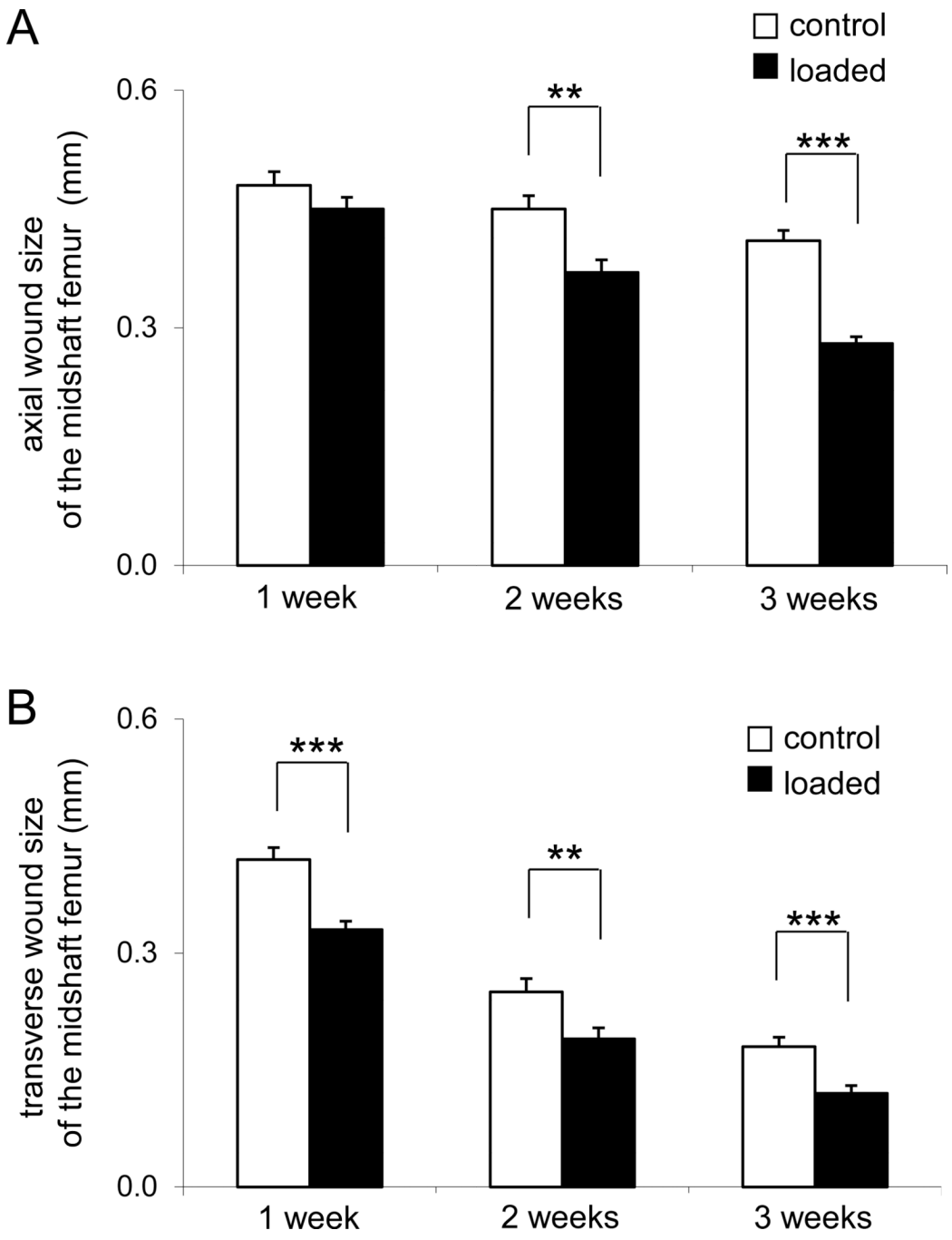

Figure 4.
Alterations in wound size in the femoral midshaft along the axial and transverse directions. (A) Wound size along the axial direction (mm). (B) Wound size along the lateral direction (mm).

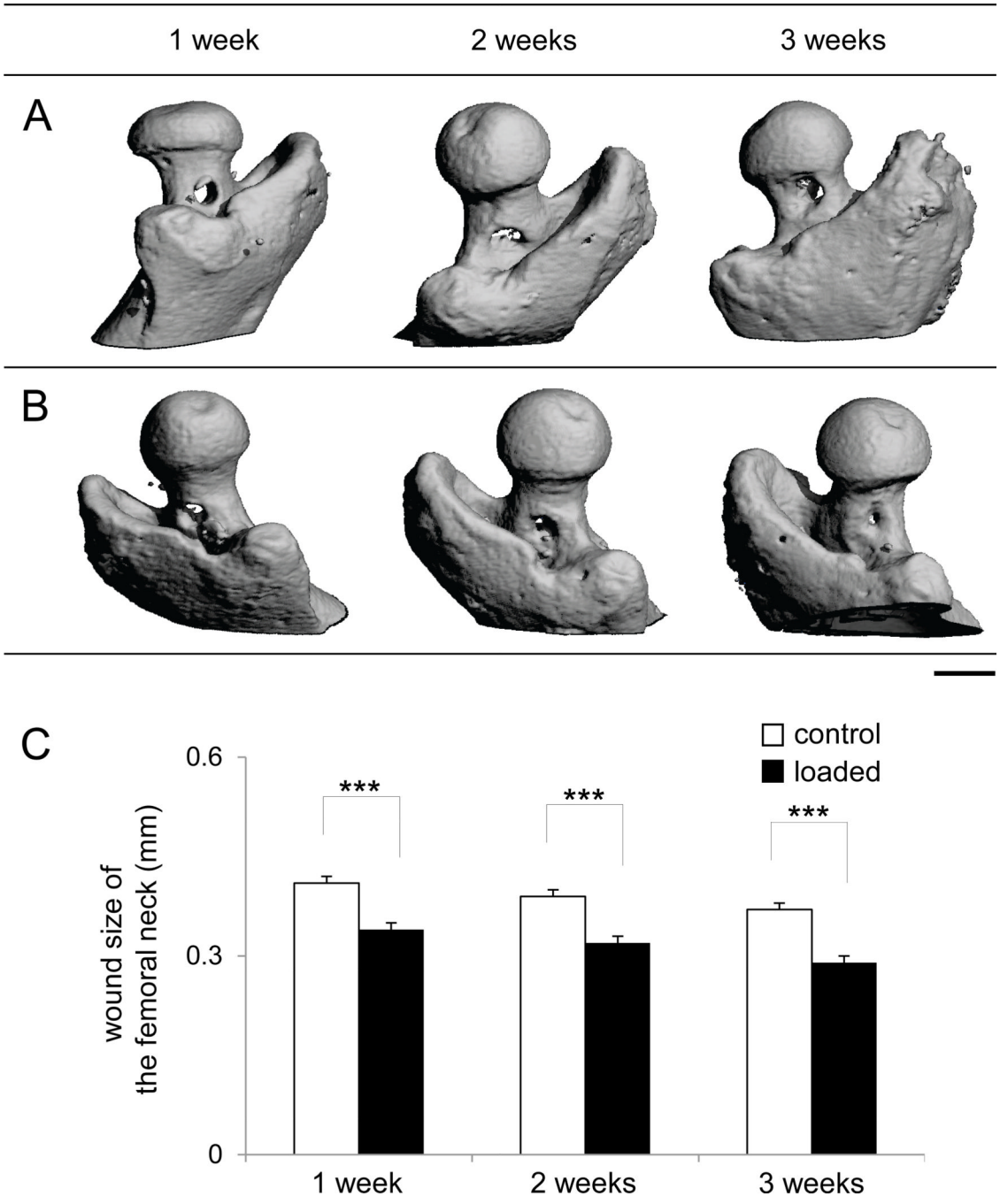

Figure 5.
Surgical wounds in the femur neck. (A) Micro CT images of the surgical holes of the control femora in the femur necks in 1, 2, and 3 weeks after surgery. (B) Micro CT images of the surgical holes of the loaded femora in the femur necks in 1, 2, and 3 weeks after surgery. Bar = 1 mm. (C) Changes in wound size in the femur neck (mm).

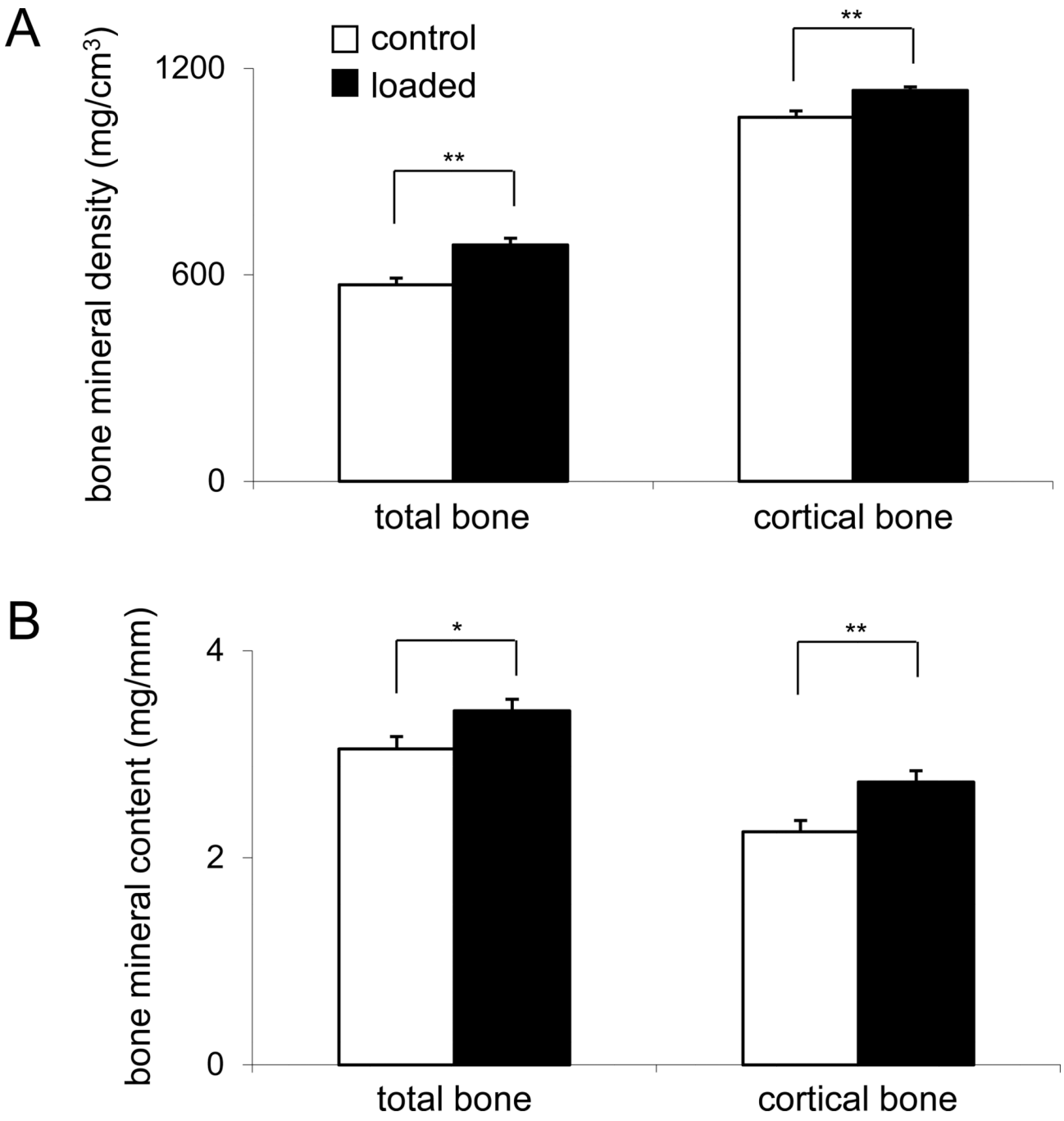

Figure 6.
Alteration in bone mineral density and bone mineral content in the third postoperative week. (A) Total BMD and cortical BMD (mg/cm^3). (B) Total BMC and cortical BMC (mg/mm).

Table 1

Summary of mechanical testing

items	unit	control	loaded	P value
stiffness	N/mm	27.83 ± 1.90	38.55 ± 4.37	0.03
ultimate force	N	11.37 ± 0.91	11.97 ± 0.58	0.30
pre-ult. force displacement	mm	0.71 ± 0.04	0.65 ± 0.06	0.23
energy to ultimate force	mJ	5.37 ± 0.71	5.25 ± 0.62	0.45